

Preparation, X-Ray Structural Analysis, and Method of Interconversion of Two Isomeric Forms of $[\text{Os}_6(\text{CO})_{16}\{\text{P}(\text{OMe})_3\}_2]^\dagger$

Brian F. G. Johnson, Rose A. Kamarudin, Fernando J. Lahoz, Jack Lewis,* and Paul R. Raithby
University Chemical Laboratory, Lensfield Road, Cambridge CB2 1EW

Treatment of the labile cluster $[\text{Os}_6(\text{CO})_{16}(\text{NCMe})_2]$ (**1**) with excess trimethyl phosphite, at room temperature, affords two isomers of $[\text{Os}_6(\text{CO})_{16}\{\text{P}(\text{OMe})_3\}_2]$ (**2a**) and (**2b**) as the major products, together with small amounts of $[\text{Os}_6(\text{CO})_{15}\{\text{P}(\text{OMe})_3\}_3]$ (**3**). The ^1H n.m.r. spectrum of (**2a**) indicates that the two $\text{P}(\text{OMe})_3$ groups are equivalent, and an X-ray analysis of this product shows that these two ligands occupy equivalent sites on the two capping Os atoms of the bicapped-tetrahedral metal framework, as has been observed previously in other disubstituted derivatives of $[\text{Os}_6(\text{CO})_{18}]$. In isomer (**2b**), ^1H n.m.r. data show that the two phosphite environments are inequivalent. This is confirmed by the X-ray crystal structure in which the bicapped tetrahedral hexaosmium framework is retained, but while one $\text{P}(\text{OMe})_3$ group occupies a site on one of the capping Os atoms, the other is co-ordinated to one of the Os atoms in the central tetrahedron. In solution isomer (**2b**) converts to (**2a**). Possible mechanisms by which this interconversion may take place are discussed.

The factors, both kinetic and thermodynamic, which govern the initial site of nucleophilic attack, and the eventual site of occupation by ligands such as phosphines and phosphites in substitution reactions of small transition metal clusters has been the subject of much recent interest.¹⁻⁴ However, for cluster complexes with a nuclearity greater than four, nucleophilic substitution reactions have not been extensively investigated, and are not well understood.

A recent development in the substitution chemistry of hexa- osmium complexes is the extension of the $\text{Me}_3\text{NO}-\text{MeCN}$ labilisation reaction⁵ to the higher nuclearity systems.^{6,7} In this way, it is possible to introduce the labile MeCN ligand into these clusters, and thus greatly enhance their reactivity under mild reactions conditions. In this paper we report the results of investigations into the nature of the substitution reactions of the labile bis-acetonitrile complex, $[\text{Os}_6(\text{CO})_{16}(\text{NCMe})_2]$ (**1**), with trimethyl phosphite. Two important features emerge. The bis-substitution product exists in two isomeric forms, in each case the basic bicapped-tetrahedral metal framework is preserved, and, because of the low symmetry of the two forms, it is possible to comment on the mechanism of both nucleophilic substitution and the isomerisation process.

Results and Discussion

The reaction of $[\text{Os}_6(\text{CO})_{18}]$ with a slight excess of Me_3NO (*ca.* 2.1 equivalents) in $\text{MeCN}-\text{CH}_2\text{Cl}_2$ at -78°C affords the bis-substituted cluster (**1**) in high yield. Attempts to purify this product by t.l.c. have only led to decomposition, but it may be used *in situ*, and has proven to be an excellent precursor for a wide range of hexa- osmium derivatives. Crystals of (**1**) suitable for X-ray analysis have not yet been obtained, and although it is presumed that the bicapped-tetrahedral metal framework geometry, observed in $[\text{Os}_6(\text{CO})_{18}]$,⁸ is retained, the site of substitution of the MeCN groups is not known.

Treatment of (**1**) with excess trimethyl phosphite, in CH_2Cl_2 ,

at room temperature, affords a compound of formula $[\text{Os}_6(\text{CO})_{16}\{\text{P}(\text{OMe})_3\}_2]$ (**2**) as the major product (75% yield) together with small amounts of the trisubstituted derivative $[\text{Os}_6(\text{CO})_{15}\{\text{P}(\text{OMe})_3\}_3]$ (**3**). Attempts at purification by t.l.c. led to the conclusion that (**2**) exists in two isomeric forms. Two close lying bands were observed on the chromatographic plate, and after elution with CH_2Cl_2 -hexane (1:3), followed by crystallisation, two very similar complexes (**2a**) and (**2b**) were obtained. Both showed the same strong molecular ion at $m/e = 1\ 848$ followed by sequential loss of 16 carbonyl ligands in their mass spectra. One isomer, (**2a**) has a $\nu(\text{CO})$ i.r. spectrum (Table 1) very similar to that observed for $[\text{Os}_6(\text{CO})_{16}(\text{PPh}_3)_2]$ ⁶ and $[\text{Os}_6(\text{CO})_{16}(\text{CNBu}^t)_2]$ ⁹ which have the structures shown in Figure 1, in which the two non-carbonyl ligands occupy sites on the two capping Os atoms of the bicapped-tetrahedral framework. The second isomer, (**2b**), has a different $\nu(\text{CO})$ i.r. pattern although generally resembling that observed for (**1**) (Table 1). The ^1H n.m.r. spectrum of (**2a**) shows a single doublet in keeping with the structure previously observed for $[\text{Os}_6(\text{CO})_{16}(\text{PPh}_3)_2]$ ⁶ (Figure 1), whereas isomer (**2b**) exhibits

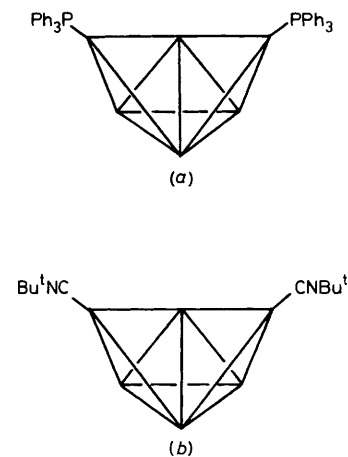


Figure 1. The structures of $[\text{Os}_6(\text{CO})_{16}(\text{PPh}_3)_2]$ (a) and $[\text{Os}_6(\text{CO})_{16}(\text{CNBu}^t)_2]$ (b)

[†] 1,1,1,2,2,2,3,3,3,4,4,4,5,5,6,6-Hexadecacarbonyl-5,6- and 1,1,1,2,2,2,3,3,3,4,4,4,5,5,6,6-Hexadecacarbonyl-4,6-bis(trimethyl phosphite)-polyhedro-hexa- osmium(12 Os-Os).

Supplementary data available: see Instructions for Authors, *J. Chem. Soc., Dalton Trans.*, 1988, Issue 1, pp. xvii-xx.

Table 1. Analytical data spectroscopic properties of $[\text{Os}_6(\text{CO})_{16}\text{L}_2]$ derivatives

Compound	I.r. (ν/cm^{-1})	^1H N.m.r. (δ)	Mass spectrum m/e	Analysis* (%)			
				C	H	N	P
$[\text{Os}_6(\text{CO})_{16}(\text{NCMe})_2]$ (1)	2 083w, 2 048m, 2 017s, 1 951w	2.77 (s, 6 H)		14.35 (14.65)	0.35 (0.60)	1.70 (1.60)	
$[\text{Os}_6(\text{CO})_{16}\{\text{P}(\text{OMe})_3\}_2]$ (2a)	2 080w, 2 071w, 2 034s, 2 024s, 1 986w, 1 965w	3.82 (d, 18 H, $J = 11.7$ Hz)	1 848	14.4 (14.2)	1.00 (1.05)		3.35 (3.50)
(2b)	2 082w, 2 043m, 2 023s, 1 969w	3.80 (d, 9 H, $J = 11.8$ Hz) 3.81 (d, 9 H, $J = 11.6$ Hz)	1 848	14.4 (14.25)	1.00 (0.95)		3.35 (3.35)

* Calculated values given in parentheses.

Table 2. Selected bond lengths (\AA) and angles ($^\circ$) for $[\text{Os}_6(\text{CO})_{16}\{\text{P}(\text{OMe})_3\}_2]$ (2a)

Os(2)–Os(1)	2.835(1)	Os(3)–Os(2)	2.799(1)	O(3)–P(1)	1.564(15)	C(22)–Os(2)	1.901(17)
Os(3)–Os(1)	2.799(1)	Os(4)–Os(2)	2.790(1)	C(41)–Os(4)	1.895(18)	C(23)–Os(2)	1.907(18)
Os(4)–Os(1)	2.898(1)	Os(5)–Os(2)	2.747(1)	C(42)–Os(4)	1.905(23)	C(31)–Os(3)	1.916(15)
Os(4)–Os(3)	2.790(1)	Os(5)–Os(4)	2.807(1)	C(43)–Os(4)	1.885(14)	C(32)–Os(3)	1.896(20)
Os(5)–Os(3)	2.784(1)	Os(6)–Os(4)	2.834(1)	C(51)–Os(5)	1.897(21)	C(33)–Os(3)	1.900(21)
Os(6)–Os(3)	2.858(1)	Os(6)–Os(5)	2.829(1)	C(52)–Os(5)	1.905(20)	Os(6)–P(2)	2.274(4)
Os(1)–P(1)	2.275(4)	C(11)–Os(1)	1.867(21)	C(53)–Os(5)	1.909(21)	O(4)–P(2)	1.579(13)
O(1)–P(1)	1.579(12)	C(12)–Os(1)	1.847(25)	C(61)–Os(6)	1.803(20)	O(5)–P(2)	1.601(15)
O(2)–P(1)	1.597(14)	C(21)–Os(2)	1.927(18)	C(62)–Os(6)	1.877(22)	O(6)–P(2)	1.562(14)
Os(3)–Os(1)–Os(2)	59.6(1)	Os(3)–Os(2)–Os(1)	59.6(1)	Os(4)–Os(5)–Os(2)	60.3(1)	Os(6)–Os(4)–Os(3)	61.1(1)
Os(4)–Os(1)–Os(2)	58.2(1)	Os(4)–Os(2)–Os(1)	62.0(1)	Os(4)–Os(5)–Os(3)	59.9(1)	Os(6)–Os(4)–Os(5)	60.2(1)
Os(4)–Os(1)–Os(3)	58.6(1)	Os(4)–Os(2)–Os(3)	59.9(1)	Os(6)–Os(5)–Os(2)	111.2(1)	Os(4)–Os(6)–Os(3)	58.7(1)
Os(2)–Os(3)–Os(1)	60.9(1)	Os(5)–Os(2)–Os(1)	111.1(1)	Os(6)–Os(5)–Os(3)	61.2(1)	Os(5)–Os(6)–Os(3)	58.6(1)
Os(4)–Os(3)–Os(1)	62.5(1)	Os(5)–Os(2)–Os(3)	60.3(1)	Os(6)–Os(5)–Os(4)	60.4(1)	Os(5)–Os(6)–Os(4)	59.4(1)
Os(4)–Os(3)–Os(2)	59.9(1)	Os(5)–Os(2)–Os(4)	60.9(1)	O(1)–P(1)–Os(1)	120.7(5)	Os(4)–P(2)–Os(6)	119.0(5)
Os(5)–Os(3)–Os(1)	111.1(1)	Os(2)–Os(4)–Os(1)	59.8(1)	O(2)–P(2)–Os(1)	110.5(5)	Os(5)–P(2)–Os(6)	109.8(4)
Os(5)–Os(3)–Os(2)	58.9(1)	Os(3)–Os(4)–Os(1)	58.9(1)	O(3)–P(1)–Os(1)	112.4(5)	O(6)–P(2)–Os(6)	112.6(5)
Os(5)–Os(3)–Os(4)	60.5(1)	Os(3)–Os(4)–Os(2)	60.2(1)	O(2)–P(1)–O(1)	102.9(7)	O(5)–P(2)–O(4)	104.4(7)
Os(6)–Os(3)–Os(1)	115.8(1)	Os(5)–Os(4)–Os(1)	107.6(1)	O(3)–P(1)–O(1)	101.0(7)	O(6)–P(2)–O(4)	100.1(7)
Os(6)–Os(3)–Os(2)	108.8(1)	Os(5)–Os(4)–Os(2)	58.8(1)	O(3)–P(1)–O(2)	108.7(8)	O(6)–P(2)–O(5)	110.3(8)
Os(6)–Os(3)–Os(4)	60.2(1)	Os(5)–Os(4)–Os(3)	59.7(1)	P(1)–Os(1)–Os(2)	108.4(1)	P(2)–Os(6)–Os(3)	161.2(1)
Os(6)–Os(3)–Os(5)	60.2(1)	Os(6)–Os(4)–Os(1)	113.5(1)	P(1)–Os(1)–Os(3)	111.8(1)	P(2)–Os(6)–Os(4)	105.3(1)
Os(3)–Os(5)–Os(2)	60.8(1)	Os(6)–Os(4)–Os(2)	109.8(1)	P(1)–Os(1)–Os(4)	165.8(1)	P(2)–Os(6)–Os(5)	105.9(1)

two sets of doublets consistent with the existence of two different $\text{P}(\text{OMe})_3$ environments (Table 1). In order to confirm the spectroscopic structural assignment for (2a) and to establish the structure of (2b) single-crystal X -ray analyses were carried out on both isomers.

The molecular structures of the isomers (2a) and (2b) are shown in Figures 2 and 3, respectively, while selected bond parameters are presented in Tables 2 and 3. In both cases the crystal structures exist as well separated hexaosmium complexes with no short intermolecular contacts.

The overall metal framework geometry and the ligand distribution found in isomer (2a) is similar to that previously observed for the other crystallographically characterised bis-substituted clusters, $[\text{Os}_6(\text{CO})_{16}(\text{PPh}_3)_2]$ ⁶ and $[\text{Os}_6(\text{CO})_{16}(\text{CN-Bu}^t)_2]$.⁹ The two phosphite ligands occupy sites on the capping metal atoms, Os(1) and Os(6), with the Os–P vectors *pseudo-trans* to the relatively long Os(1)–Os(4) and Os(3)–Os(6) vectors, in such an arrangement that the molecule has approximate C_2 symmetry. Except for the two metal–metal bonds *trans* to the phosphite ligands, the Os–Os bond distances follow the same trends as in other bicapped tetrahedral structures.^{6,8–10} In terms of electron counting, the six metal atoms are formally associated with different numbers of electrons, introducing polarity into the metal framework. The capping metal atoms, Os(1) and Os(6), with three metal contacts formally only have 17 electrons each. The metals, Os(2) and Os(5), with four metal contacts, are each associated with 18 electrons, while the

remaining two metals, Os(3) and Os(4), with five metal contacts, are formally electron rich with 19 electrons each.

The shortest metal–metal distance in the structure is between the two 18-electron Os atoms, and is similar in length to that found in $[\text{Os}_6(\text{CO})_{18}]$ [2.732(1) \AA]⁸ and $[\text{Os}_6(\text{CO})_{17}(\text{PPh}_3)]$ [2.743(4) \AA].⁶ The variation of metal–metal distances within the caps also follows the trend observed for $[\text{Os}_6(\text{CO})_{16}(\text{PPh}_3)_2]$,⁶ where the range is 2.781(1)–2.943(1) \AA . However, the increase in the Os–Os distance *trans* to the phosphorus donor ligand is not as great in the case of the bis-phosphite as in the bis-phosphine complex, the distance for this metal–metal bond in $[\text{Os}_6(\text{CO})_{16}(\text{PPh}_3)_2]$ being *ca.* 0.06 \AA longer than the average distance of 2.88(1) \AA for the two equivalent bonds in $[\text{Os}_6(\text{CO})_{16}\{\text{P}(\text{OMe})_3\}_2]$ (2a).

The Os–P distances in the phosphite derivative (2a) are *ca.* 0.09 \AA shorter than the Os–P(phosphine) distances [average 2.366(5) \AA] in $[\text{Os}_6(\text{CO})_{17}(\text{PPh}_3)]$ and $[\text{Os}_6(\text{CO})_{16}(\text{PPh}_3)_2]$.⁶ However, the Os–P distances in (2a) are similar to the range of Os–P(phosphite) lengths [2.227(12)–2.268(8) \AA] in the phosphite-substituted 'raft' complex $[\text{Os}_6(\text{CO})_{17}\{\text{P}(\text{OMe})_3\}_4]$.¹¹ The difference in these Os–Os and Os–P distances between the phosphite and phosphine derivatives reflects the somewhat different donor–acceptor properties of these phosphorus donor ligands.

The electron imbalance within the cluster framework of (2a) is also indicated by the network of incipient bridging carbonyls the dimensions of which are listed in Table 4. As has been

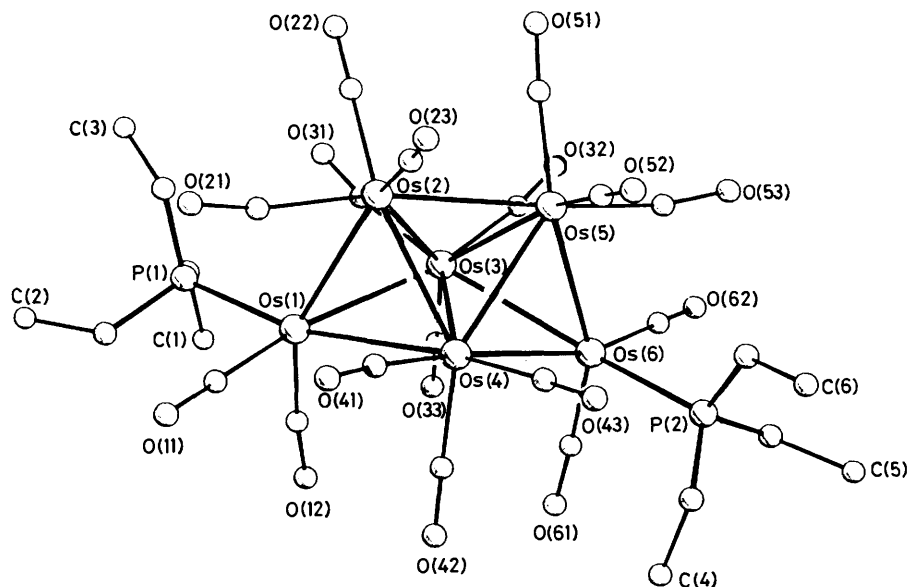


Figure 2. The molecular structure of $[\text{Os}_6(\text{CO})_{16}\{\text{P}(\text{OMe})_3\}_2]$ (**2a**) showing the numbering scheme adopted

Table 3. Selected bond lengths (Å) and angles (°) for $[\text{Os}_6(\text{CO})_{16}\{\text{P}(\text{OMe})_3\}_2]$ (**2b**)

Os(2)–Os(1)	2.820(1)	Os(3)–Os(2)	2.812(1)	O(3)–P(1)	1.582(21)	C(22)–Os(2)	1.851(24)
Os(3)–Os(1)	2.777(1)	Os(4)–Os(4)	2.788(1)	C(41)–Os(4)	1.887(29)	C(23)–Os(2)	1.905(27)
Os(4)–Os(1)	2.934(2)	Os(5)–Os(2)	2.751(2)	C(42)–Os(4)	1.913(22)	C(31)–Os(3)	1.888(29)
Os(4)–Os(3)	2.797(1)	Os(5)–Os(4)	2.841(1)	C(43)–Os(4)	1.904(29)	C(32)–Os(3)	1.872(27)
Os(5)–Os(3)	2.798(1)	Os(6)–Os(4)	2.754(1)	C(52)–Os(5)	1.887(29)	C(33)–Os(3)	1.965(25)
Os(6)–Os(3)	2.844(1)	Os(6)–Os(5)	2.819(1)	C(53)–Os(5)	1.851(27)	Os(5)–P(2)	2.310(6)
Os(1)–P(1)	2.260(8)	C(11)–Os(1)	1.805(31)	C(61)–Os(6)	1.848(21)	O(4)–P(2)	1.587(20)
O(1)–P(1)	1.517(23)	C(12)–Os(1)	1.860(22)	C(62)–Os(6)	1.901(28)	O(5)–P(2)	1.541(19)
O(2)–P(1)	1.585(24)	C(21)–Os(2)	1.861(32)	C(63)–Os(6)	1.879(30)	O(6)–P(2)	1.519(21)
Os(3)–Os(1)–Os(2)	60.3(1)	Os(3)–Os(2)–Os(1)	59.1(1)	Os(4)–Os(5)–Os(3)	59.5(1)	Os(6)–Os(4)–Os(5)	60.5(1)
Os(4)–Os(1)–Os(2)	57.9(1)	Os(4)–Os(2)–Os(1)	63.1(1)	Os(6)–Os(5)–Os(2)	109.5(1)	Os(4)–Os(6)–Os(3)	59.9(1)
Os(4)–Os(1)–Os(3)	58.6(1)	Os(4)–Os(2)–Os(3)	59.9(1)	Os(6)–Os(5)–Os(3)	60.8(1)	Os(5)–Os(6)–Os(3)	59.2(1)
Os(2)–Os(3)–Os(1)	60.6(1)	Os(5)–Os(2)–Os(1)	111.9(1)	Os(6)–Os(5)–Os(4)	58.2(1)	Os(5)–Os(6)–Os(4)	61.3(1)
Os(4)–Os(3)–Os(1)	63.5(1)	Os(5)–Os(2)–Os(3)	60.4(1)	O(1)–P(1)–Os(1)	123.4(12)	O(4)–P(2)–Os(5)	117.1(7)
Os(4)–Os(3)–Os(2)	59.6(1)	Os(5)–Os(2)–Os(4)	61.7(1)	O(2)–P(1)–Os(1)	109.2(10)	O(5)–P(2)–Os(5)	113.3(7)
Os(5)–Os(3)–Os(1)	111.8(1)	Os(2)–Os(4)–Os(1)	59.0(1)	O(3)–P(1)–Os(1)	115.0(11)	O(6)–P(2)–Os(5)	115.4(6)
Os(5)–Os(3)–Os(2)	58.7(1)	Os(3)–Os(4)–Os(1)	57.9(1)	O(2)–P(1)–O(1)	103.0(15)	O(5)–P(2)–O(4)	104.3(9)
Os(5)–Os(3)–Os(4)	61.0(1)	Os(3)–Os(4)–Os(2)	60.5(1)	O(3)–P(1)–O(1)	101.2(13)	O(6)–P(2)–O(4)	99.7(10)
Os(6)–Os(3)–Os(1)	115.6(1)	Os(5)–Os(4)–Os(1)	106.1(1)	O(3)–P(1)–O(2)	102.5(14)	O(6)–P(2)–O(5)	105.3(11)
Os(6)–Os(3)–Os(2)	107.0(1)	Os(5)–Os(4)–Os(2)	58.5(1)	P(1)–Os(1)–Os(2)	108.7(2)	P(2)–Os(5)–Os(2)	90.2(2)
Os(6)–Os(3)–Os(4)	58.5(1)	Os(5)–Os(4)–Os(3)	59.5(1)	P(1)–Os(1)–Os(3)	115.1(2)	P(2)–Os(5)–Os(3)	106.5(2)
Os(6)–Os(3)–Os(5)	59.9(1)	Os(6)–Os(4)–Os(1)	113.5(1)	P(1)–Os(1)–Os(4)	166.6(2)	P(2)–Os(5)–Os(4)	150.0(2)
Os(3)–Os(5)–Os(2)	60.9(1)	Os(6)–Os(4)–Os(2)	110.2(1)			P(2)–Os(5)–Os(6)	142.0(2)
Os(4)–Os(5)–Os(2)	59.8(1)	Os(6)–Os(4)–Os(3)	61.6(1)				

previously discussed in detail,¹² incipient carbonyl bridge bonding is usually observed between metal atoms with different formal electron counts. A carbonyl group which is bound to a formally electron-rich metal bends towards an adjacent electron-poor metal. The 'interaction' is characterised by relatively short Os...C contacts and deviations from linearity of the carbonyl groups. As in the bis-phosphine derivative $[\text{Os}_6(\text{CO})_{16}(\text{PPh}_3)_2]$,⁶ each of the capping atoms in (**2a**) [Os(1) and Os(6) (17 electrons)] is involved in a short incipient bridge with a carbonyl ligand co-ordinated to an 18-electron metal atom [Os(2) and Os(5)]. There are also slightly longer contacts between carbonyls co-ordinated to the formally 19-electron Os atoms [Os(3) and Os(4)] and the 18- and 17-electron metal atoms.

The bicapped-tetrahedral metal geometry observed in the structure of (**2a**) is retained in the structure of isomer (**2b**). However, consistent with the ¹H n.m.r. data, the two phosphite ligands occupy two inequivalent sites. One is co-ordinated to one of the capping Os atoms, Os(1), and lies pseudo-*trans* to the long Os(1)–Os(4) edge. The other is co-ordinated to one of the metal atoms in the central tetrahedron, Os(5), on the opposite side of the cluster to the phosphine-substituted cap. The Os(5)–P(2) vector lies approximately perpendicular to the Os(2)Os(3)Os(5) plane. Despite the different distribution of the phosphites each metal remains co-ordinated to three ligands, and the formal electron count is as in isomer (**2a**).

The overall trends in metal–metal distances resemble those in the other bicapped-tetrahedral structures.^{6,8–10} In (**2b**) the

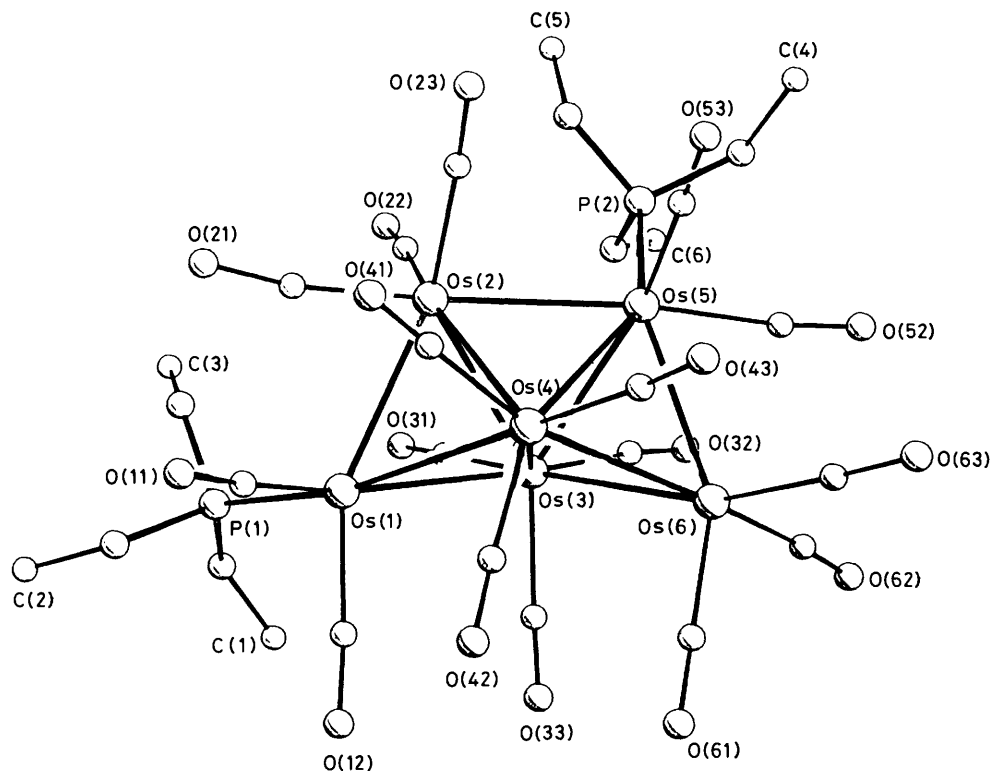


Figure 3. The molecular structure of $[\text{Os}_6(\text{CO})_{16}\{\text{P}(\text{OMe})_3\}_2]$ (**2b**) showing the numbering scheme adopted

Table 4. Intramolecular short contacts (Å) and associated M–C–O angles (°) for $[\text{Os}_6(\text{CO})_{16}\{\text{P}(\text{OMe})_3\}_2]$ (**2a**)

	Os...C	Os–C–O
Os(1)...C(21)	2.70(2)	164(2)
Os(1)...C(31)	3.04(2)	171(2)
Os(2)...C(41)	3.01(2)	174(1)
Os(5)...C(32)	3.02(2)	172(1)
Os(6)...C(32)	3.11(2)	172(1)
Os(6)...C(53)	2.74(2)	168(2)

Table 5. Intramolecular short contacts (Å) and associated M–C–O angles (°) for $[\text{Os}_6(\text{CO})_{16}\{\text{P}(\text{OMe})_3\}_2]$ (**2b**)

	Os...C	Os–C–O
Os(1)...C(21)	2.79(2)	171(2)
Os(1)...C(31)	3.05(2)	174(3)
Os(2)...C(41)	2.94(2)	176(3)
Os(5)...C(32)	2.94(2)	173(2)
Os(6)...C(43)	2.95(2)	173(3)
Os(6)...C(52)	2.76(2)	172(2)

variation in Os–Os distances in the phosphite-substituted cap are greater than in the caps in (**2a**), and the Os(1)–Os(4) bond *trans* to the phosphite, in particular, is *ca.* 0.06 Å longer than the equivalent distances in (**2a**), and more in keeping with the value of 2.943(1) Å found in $[\text{Os}_6(\text{CO})_{16}(\text{PPh}_3)_2]$.⁶ The distances within the non-substituted cap, centred on Os(6) show a much smaller variation more in keeping with the range of distances [2.780(1)–2.836(1) Å] found in the caps of $[\text{Os}_6(\text{CO})_{18}]$.⁸ The distance between the two formally 18-electron atoms, Os(2)–Os(5), remains the shortest metal–metal interaction in the structure of (**2b**) and is not significantly different from the value in (**2a**). The introduction of the phosphite ligand into the co-ordination sphere of Os(5) has caused a slight increase (*ca.* 0.025 Å) in the Os(3)–Os(5) and Os(4)–Os(5) distances over those in isomer (**2a**). This is consistent with the greater donating properties of the phosphite over the carbonyl ligand. The Os(5)–P(2) bond length is 0.05 Å longer than the Os(1)–P(1) distance for the phosphite co-ordinated to the capping Os(1) atom. While the Os(1)–P(1) length in (**2b**) is similar to the equivalent distances in (**2a**), the Os(5)–P(2) length is more reminiscent of the Os–P(phosphine) distance of 2.368(3) Å in the bis-phosphine complex $[\text{Os}_6(\text{CO})_{16}(\text{PPh}_3)_2]$.⁶

As in (**2a**) a network of incipient bridging carbonyls is present in the structure of (**2b**). The relevant Os...C and Os–C–O parameters for (**2b**) are presented in Table 5. Despite the change in position of the second phosphite in (**2b**) there are only relatively small changes in the distribution of the incipient bridges compared to (**2a**), and as in (**2a**) there are two short contacts between the capping Os(1) and Os(6) (17 electrons) and the carbonyls co-ordinated to the 18-electron atoms [Os(2) and Os(5)]. There are slightly longer contacts between the carbonyls co-ordinated to the 19-electron metals [Os(3) and Os(4)] and the 18- and 17-electron metal atoms.

In solution isomer (**2b**) converts into (**2a**) indicating that the structure with the substituted ligands occupying sites on the capping metal atoms is thermodynamically more favourable. This is also considered to be the preferential arrangement for the kinetic product of the direct substitution reactions of the parent cluster, $[\text{Os}_6(\text{CO})_{18}]$. Since the capping Os atoms, with a formal 17-electron count, may be regarded as the most electron-deficient site within the molecule this is perfectly understandable. However, from the similarity of the i.r. spectra of (**1**) and (**2b**) (Table 1), it is possible that one of the MeCN ligands in (**1**) occupies a site on one of the Os atoms in the

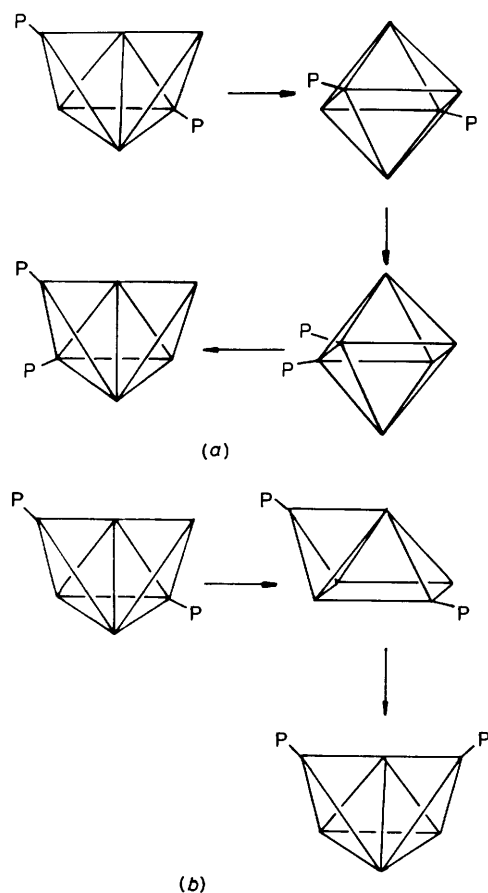


Figure 4. Possible mechanisms for the transformation of isomer (**2a**) into isomer (**2b**). (a) Pathway involving an octahedral intermediate which would give a *cis* product. (b) Pathway involving a capped square-pyramidal intermediate which gives the observed product

central tetrahedron. This apparently anomalous behaviour is almost certainly a reflection on the method by which $[\text{Os}_6(\text{CO})_{16}(\text{MeCN})_2]$ (**1**) was prepared. Replacement of CO by MeCN occurs *via* the initial electrophilic attack of Me_3NO on a co-ordinated carbon monoxide ligand.⁵ The site of electrophilic attack cannot be predicted with certainty, but it is likely to be different to that of nucleophilic addition.

Although it is not possible, at this stage, to determine the mechanism of isomerisation, it has been established that any dissociative process involving the migration of $\text{P}(\text{OMe})_3$ groups may be excluded. Thus, the ^1H n.m.r. spectrum of either isomer shows no evidence for phosphite dissociation under the conditions of isomerisation. In line with previous discussions on polyhedral rearrangements in metal clusters¹³ it is believed that the mechanism by which isomerisation occurs almost certainly involves single edge cleavage. On these grounds two possible mechanisms may be considered. First, the rearrangement could occur *via* an octahedral Os_6 intermediate. However, this mechanism maintains the *cis* arrangement of the $\text{P}(\text{OMe})_3$ ligands throughout (Figure 4). The second possible rearrangement pathway is conversion *via* a monocapped square-pyramidal intermediate as shown in Figure 4. The appropriate isomer interchange can occur by this route.

Experimental

None of the compounds reported here is air-sensitive, but all reactions were carried out under an atmosphere of dry nitrogen. Products were separated in the air by thin-layer chromatography (t.l.c.) with plates coated with Merck Kieselgel 60 F₂₅₄ (0.25 mm thick). All solvents were dried over appropriate reagents and distilled prior to use.

Proton n.m.r. data were obtained on Bruker WM250 or Varian XL100 instruments at 20 °C using deuteriated solvents as lock and reference (SiMe_4 , $\delta = 0$). Infrared spectra were recorded on a Perkin-Elmer 983 spectrometer between 2 140 and 1 600 cm^{-1} using CO (g) as calibrant. Mass spectra were obtained on an AEI MS12 spectrometer with *ca.* 70 eV ($1.12 \times$

Table 6. Atomic co-ordinates ($\times 10^4$) for $[\text{Os}_6(\text{CO})_{16}\{\text{P}(\text{OMe})_3\}_2]$ (**2a**)

Atom	x	y	z	Atom	x	y	z
Os(1)	6 323(1)	8 686(1)	6 398(1)	C(51)	8 027(21)	8 597(19)	9 240(12)
Os(2)	8 002(1)	8 157(1)	7 577(1)	C(52)	10 830(22)	10 426(18)	8 821(11)
Os(3)	5 926(1)	9 417(1)	7 795(1)	C(53)	8 640(19)	11 076(17)	9 434(11)
Os(4)	8 759(1)	10 633(1)	7 208(1)	P(2)	9 660(5)	13 733(4)	8 514(3)
Os(5)	8 652(1)	9 983(1)	8 647(1)	O(4)	10 612(12)	14 492(10)	7 892(7)
Os(6)	7 643(1)	11 947(1)	8 228(1)	O(5)	9 056(14)	14 706(10)	8 927(8)
P(1)	4 407(5)	6 894(4)	6 012(3)	O(6)	10 988(13)	13 504(11)	8 972(7)
O(1)	2 659(12)	6 695(11)	6 145(7)	C(4)	9 899(19)	15 036(17)	7 339(11)
O(2)	4 395(14)	6 716(13)	5 162(7)	C(5)	10 096(23)	15 921(20)	9 219(13)
O(3)	4 586(13)	5 721(11)	6 361(8)	C(6)	12 638(24)	14 319(21)	9 049(13)
C(1)	1 939(23)	7 562(20)	5 888(13)	O(21)	8 159(13)	6 527(12)	6 291(7)
C(2)	3 345(24)	5 641(21)	4 726(14)	O(22)	6 287(14)	5 794(11)	8 323(9)
C(3)	3 440(23)	4 517(20)	6 491(13)	O(23)	11 298(13)	8 275(12)	7 922(8)
O(11)	7 884(16)	8 455(17)	5 047(8)	O(41)	10 602(14)	9 731(13)	6 152(7)
O(12)	4 802(22)	10 360(17)	5 711(8)	O(42)	8 090(19)	12 355(15)	6 133(11)
O(31)	3 557(13)	6 796(11)	7 742(8)	O(43)	11 978(13)	12 438(12)	7 658(9)
O(32)	4 737(15)	9 406(15)	9 287(8)	O(61)	6 154(15)	13 300(13)	7 245(8)
O(33)	3 703(13)	10 619(12)	7 188(9)	O(62)	5 867(16)	12 549(13)	9 406(8)
O(51)	7 572(16)	7 802(12)	9 630(8)	C(21)	7 928(17)	7 176(15)	6 714(10)
O(52)	12 127(13)	10 704(13)	8 922(9)	C(22)	6 924(18)	6 684(16)	8 048(10)
O(53)	8 637(14)	11 576(12)	9 984(8)	C(23)	10 078(18)	8 263(15)	7 815(10)
C(11)	7 272(19)	8 528(16)	5 557(11)	C(41)	9 860(17)	10 009(15)	6 555(10)
C(12)	5 357(23)	9 664(20)	5 951(13)	C(42)	8 273(21)	11 692(19)	6 542(12)
C(31)	4 466(17)	7 753(16)	7 702(10)	C(43)	10 718(18)	11 771(16)	7 521(10)
C(32)	5 228(18)	9 504(16)	8 728(11)	C(61)	6 764(18)	12 781(16)	6 748(11)
C(33)	4 555(19)	10 191(16)	7 416(11)	C(62)	6 563(20)	12 329(18)	8 975(12)

Table 7. Atomic co-ordinates ($\times 10^4$) for $[\text{Os}_6(\text{CO})_{16}\{\text{P}(\text{OMe})_3\}_2]$ (**2b**)

Atom	x	y	z	Atom	x	y	z
Os(1)	7 251(1)	8 302(1)	11 010(1)	C(31)	6 770(14)	5 704(30)	10 117(12)
Os(2)	6 567(1)	9 030(1)	9 722(1)	C(32)	7 565(12)	5 428(28)	9 425(12)
Os(3)	7 566(1)	6 753(1)	10 064(1)	C(33)	8 288(15)	5 741(31)	10 759(13)
Os(4)	8 019(1)	9 650(1)	10 229(1)	P(2)	6 442(3)	7 563(7)	8 189(3)
Os(5)	7 416(1)	8 467(1)	8 988(1)	O(4)	6 524(9)	7 359(19)	7 508(8)
Os(6)	8 795(1)	7 696(1)	9 781(1)	O(5)	5 767(8)	8 504(23)	8 063(8)
P(1)	6 449(4)	7 237(8)	11 393(3)	O(6)	6 215(9)	6 034(22)	8 297(8)
O(1)	6 462(14)	5 633(24)	11 553(12)	C(4)	6 636(14)	8 642(31)	7 134(13)
O(2)	6 477(12)	8 002(30)	12 039(9)	C(5)	5 081(15)	8 186(34)	7 608(14)
O(3)	5 642(11)	7 446(26)	10 968(13)	C(6)	5 977(21)	4 718(48)	7 855(20)
C(1)	6 927(19)	4 571(45)	11 671(18)	O(41)	7 317(10)	12 464(21)	10 421(11)
C(2)	6 093(22)	7 553(51)	12 455(21)	O(42)	9 118(9)	9 780(21)	11 550(8)
C(3)	5 058(19)	6 658(41)	10 687(17)	O(43)	8 866(9)	11 703(19)	9 667(8)
O(11)	7 199(11)	11 031(23)	11 754(9)	O(52)	8 215(9)	7 169(22)	8 182(8)
O(12)	8 415(9)	7 089(25)	12 139(8)	O(53)	7 414(12)	11 357(22)	8 350(10)
O(21)	5 768(10)	10 622(21)	10 492(8)	O(61)	9 932(9)	7 448(21)	11 064(8)
O(22)	5 253(9)	7 166(25)	9 128(9)	O(62)	9 264(10)	4 923(21)	9 350(10)
O(23)	6 076(11)	11 531(23)	8 789(10)	O(63)	9 734(10)	9 295(24)	9 157(10)
O(31)	6 292(9)	4 963(19)	10 117(9)	C(41)	7 561(14)	11 368(31)	10 351(12)
O(32)	7 570(9)	4 471(23)	9 063(8)	C(42)	8 701(12)	9 748(27)	11 066(12)
O(33)	8 661(10)	5 023(23)	11 114(10)	C(43)	8 564(13)	10 853(29)	9 864(12)
C(11)	7 206(14)	9 883(33)	11 476(13)	C(52)	7 958(12)	7 647(28)	8 518(12)
C(12)	7 979(13)	7 527(27)	11 692(12)	C(53)	7 415(12)	10 228(30)	8 585(12)
C(21)	6 119(14)	9 947(32)	10 234(13)	C(61)	9 487(12)	7 491(26)	10 569(12)
C(22)	5 759(13)	7 940(28)	9 327(11)	C(62)	9 085(12)	5 948(30)	9 482(11)
C(23)	6 252(13)	10 553(31)	9 114(13)	C(63)	9 391(13)	8 723(29)	9 426(12)

10^{-17} J) ionizing potential at 100–150 °C. Tris(perfluoroheptyl)-s-triazine was used as solvent.

Preparation of $[\text{Os}_6(\text{CO})_{16}(\text{NCMe})_2]$ (1).—The compound $[\text{Os}_6(\text{CO})_{18}]$ (112 mg) was dissolved in CH_2Cl_2 (50 cm^3) containing MeCN (4 cm^3) and stirred at -78 °C. A solution of Me_3NO in CH_2Cl_2 (11.2 mg, 2 mol equiv.) was added dropwise into the cooled solution using a pressure-equalized dropping funnel. After all the Me_3NO solution had been added, the reaction mixture was left to warm up to room temperature. The solution was filtered through silica to remove excess Me_3NO and the filtrate was evaporated to dryness. The residue was crystallized from CH_2Cl_2 –hexane at 0 °C over a few days (yield 51%).

Reactions of (1) with $\text{P}(\text{OMe})_3$.—Pure compound (1) (25 mg) was dissolved in CH_2Cl_2 (50 cm^3) and $\text{P}(\text{OMe})_3$ (10 drops) was added. The solution was left to stir at room temperature for 1.5 h after which spot t.l.c. indicated no starting material remaining. Solvent was removed under vacuum and the brown residue was chromatographed by t.l.c. using hexane– CH_2Cl_2 (60:40) to afford $[\text{Os}_6(\text{CO})_{16}\{\text{P}(\text{OMe})_3\}_2]$ (**2a**) and (**2b**) (yield 75%) and small amounts of $[\text{Os}_6(\text{CO})_{15}\{\text{P}(\text{OMe})_3\}_3]$ (**3**) (isomers). The band containing (**2a**) and (**2b**) was rechromatographed in hexane– CH_2Cl_2 (75:25) to separate the isomers.

Crystal Structure Determination of $[\text{Os}_6(\text{CO})_{16}\{\text{P}(\text{OMe})_3\}_2]$ (2a**).**—A suitable single crystal was obtained by recrystallization from hexane solution, and was mounted on a glass fibre with epoxy-resin.

Crystal data. $\text{C}_{22}\text{H}_{18}\text{O}_{22}\text{Os}_6\text{P}_2$, $M = 1\ 837.50$, triclinic, $a = 9.214(2)$, $b = 11.451(3)$, $c = 18.699(5)$ Å, $\alpha = 91.52(3)$, $\beta = 92.45(2)$, $\gamma = 110.08(2)^\circ$, $U = 1\ 849.5$ Å³ [by least-squares refinement on diffractometer angles for 56 automatically centred reflections ($20 < 2\theta < 25^\circ$), $\lambda = 0.710\ 69$ Å], space group $P\bar{1}$ (no. 2), $Z = 2$, $D_c = 3.298$ g cm^{-3} , $F(000) = 1\ 624$. Purple multifaceted plates, crystal dimensions (distance to faces from

centre): 0.019 ($001, 00\bar{1}$) \times 0.129 ($010, 0\bar{1}0$) \times 0.181 ($10\bar{1}, \bar{1}01$) \times 0.133 ($2\bar{3}\bar{1}$) \times 0.144 ($2\bar{1}0$) mm, $\mu(\text{Mo-K}\alpha) = 206.84$ cm^{-1} .

Data collection and processing.¹⁴ Stoe-Siemens diffractometer, ω – θ scan mode with scan width of 0.05° , 24 steps in scan, scan time 0.75–3.0 s per step, graphite-monochromated Mo– $K\alpha$ radiation. 5 119 Reflections measured ($5.0 < 2\theta < 45.0^\circ$, $\pm h$, $\pm k$, $\pm l$), 4 826 unique [merging $R = 0.020$ after absorption correction (maximum, minimum transmission factors 0.462, 0.040)] giving 4 092 with $F > 4\sigma(F)$; no appreciable variation in intensity during data collection.

Structure analysis and refinement. Direct methods (Os atoms) followed by Fourier difference techniques. Blocked full-matrix least-squares refinement with Os, P, and O atoms assigned anisotropic thermal parameters. The weighting scheme $w = 3.65/[\sigma^2(F_o) + 0.0005|F_o|^2]$ gave satisfactory agreement analyses; final R and R' 0.038 and 0.038. The structure was solved and refined using SHELX 76¹⁵ and scattering factors were taken from ref. 16. Final atomic co-ordinates are listed in Table 6.

Crystal Structure Determination of $[\text{Os}_6(\text{CO})_{16}\{\text{P}(\text{OMe})_3\}_2]$ (2b**).**—A single crystal of (**2b**) was obtained by slow recrystallization from hexane solution, and was mounted on a glass fibre with epoxy-resin.

Crystal data. $\text{C}_{22}\text{H}_{18}\text{O}_{22}\text{Os}_6\text{P}_2$, $M = 1\ 837.50$, monoclinic, $a = 19.844(5)$, $b = 9.197(2)$, $c = 22.242(6)$ Å, $\beta = 109.09(2)^\circ$, $U = 3\ 836.0$ Å³ [by constrained least-squares refinement on diffractometer angles for 52 automatically centred reflections ($20 < 2\theta < 25^\circ$), $\lambda = 0.710\ 69$ Å], space group $P2_1/n$ (alternative $P2_1/c$, no. 14), $Z = 4$, $D_c = 3.181$ g cm^{-3} , $F(000) = 3\ 248$. Purple tablets, crystal dimensions (distance to faces from centre): 0.073 ($10\bar{1}, \bar{1}01$) \times 0.106 ($100, \bar{1}00$) \times 0.198 ($11\bar{1}, \bar{1}\bar{1}1$) \times 0.205 ($1\bar{1}\bar{1}, \bar{1}11$) mm, $\mu(\text{Mo-K}\alpha) = 199.45$ cm^{-1} .

Data collection and processing.¹⁴ Stoe-Siemens diffractometer, ω – θ scan mode with scan width 0.05° , 24 steps in scan, step time 0.75–3.0 s per step, graphite-monochromated Mo– $K\alpha$ radiation; 9 203 reflections measured ($5.0 < 2\theta < 42.0^\circ$, $\pm h$, $\pm k$, $\pm l$), 4 119 unique [merging $R = 0.046$ after absorption correction (maximum, minimum transmission factors 0.123,

0.044)] giving 3 544 with $F > 4\sigma(F)$. No appreciable variation in intensity during data collection.

Structure analysis and refinement. Direct methods (Os atoms) followed by Fourier difference techniques. Blocked full-matrix least-squares refinement with Os, P, and O atoms assigned anisotropic thermal parameters. The weighting scheme $w = 6.107/[\sigma^2(F_o) + 0.0001|F_o|^2]$ gave satisfactory agreement analyses; final R and R' 0.043 and 0.039. The structure was solved and refined using SHELX 76¹⁵ and scattering factors were taken from ref. 16. Final atomic co-ordinates are presented in Table 7. Additional material available from the Cambridge Crystallographic Data Centre comprises thermal parameters and remaining bond lengths and angles.

Acknowledgements

We thank the S.E.R.C. for financial support, the Universiti Teknologi Malaysia for study leave and the Tunku Abdul Rahman Foundation for financial support (for R. A. K.).

References

- D. J. Darensbourg and M. J. Incurria, *Inorg. Chem.*, 1980, **19**, 2585; D. C. Sonnenberger and J. D. Atwood, *Organometallics*, 1982, **1**, 694; D. C. Sonnenberger and J. D. Atwood, *J. Am. Chem. Soc.*, 1982, **104**, 2113; D. J. Darensbourg and B. J. Baldwin-Zuschke, *ibid.*, p. 3906; D. J. Darensbourg and D. J. Zalewski, *Inorg. Chem.*, 1984, **23**, 4382; D. J. Darensbourg and D. J. Zalewski, *Organometallics*, 1985, **4**, 92.
- M. G. Richmond and J. K. Kochi, *Inorg. Chem.*, 1986, **25**, 656.
- A. Shojaja and J. D. Atwood, *Organometallics*, 1985, **4**, 187.
- B. Ambwani, S. Chawla, and A. Pöe, *Inorg. Chem.*, 1985, **24**, 2635; K. Dahlinger, F. Falcone, and A. J. Pöe, *Inorg. Chem.*, 1986, **25**, 2654; A. Pöe and V. C. Sekhar, *J. Am. Chem. Soc.*, 1986, **108**, 3673.
- B. F. G. Johnson, J. Lewis, and D. A. Pippard, *J. Chem. Soc., Dalton Trans.*, 1981, 407; M. Tachikawa and J. R. Shapley, *J. Organomet. Chem.*, 1977, **124**, C19.
- C. Couture, D. H. Farrar, M. P. Gómez-Sal, B. F. G. Johnson, R. A. Kamarudin, J. Lewis, and P. R. Raithby, *Acta Crystallogr., Sect. C*, 1986, **42**, 163.
- C. Couture and D. H. Farrar, *J. Chem. Soc., Chem. Commun.*, 1985, 197; *J. Chem. Soc., Dalton Trans.*, 1986, 1395.
- R. Mason, K. M. Thomas, and D. M. P. Mingos, *J. Am. Chem. Soc.*, 1973, **95**, 3802.
- A. G. Orpen and G. M. Sheldrick, *Acta Crystallogr., Sect. B*, 1978, **34**, 1989.
- M. P. Gómez-Sal, B. F. G. Johnson, R. A. Kamarudin, J. Lewis, and P. R. Raithby, *J. Chem. Soc., Chem. Commun.*, 1985, 1622.
- R. J. Goudsmit, B. F. G. Johnson, J. Lewis, P. R. Raithby, and K. H. Whitmire, *J. Chem. Soc., Chem. Commun.*, 1982, 640.
- C. R. Eady, P. D. Gavens, B. F. G. Johnson, J. Lewis, M. C. Malatesta, M. J. Mays, A. G. Orpen, V. A. Rivera, G. M. Sheldrick, and M. B. Hursthouse, *J. Organomet. Chem.*, 1978, **149**, C43.
- B. F. G. Johnson, *J. Chem. Soc., Chem. Commun.*, 1986, 27.
- B. F. G. Johnson, J. Lewis, P. R. Raithby, S. N. A. B. Syed-Mustaffa, M. J. Taylor, K. H. Whitmire, and W. Clegg, *J. Chem. Soc., Dalton Trans.*, 1984, 2111.
- G. M. Sheldrick, SHELX 76, Crystal Structure Solving Package, University of Cambridge, 1976.
- 'International Tables for X-Ray Crystallography,' Kynoch Press, Birmingham, 1974, vol. 4.

Received 6th August 1987; Paper 7/1459